

Mechanism Insights into the Iridium(III)- and $B(C_6F_5)_3$ -Catalyzed Reduction of CO_2 to the Formaldehyde Level with Tertiary Silanes

Jefferson Guzmán, Asier Urriolabeitia, Marina Padilla, Pilar García-Orduña, Víctor Polo, and Francisco J. Fernández-Alvarez*



Cite This: *Inorg. Chem.* 2022, 61, 20216–20221



Read Online

ACCESS |



Metrics & More



Article Recommendations



Supporting Information

ABSTRACT: The catalytic system $[Ir(CF_3CO_2)(\kappa^2-NSi^{Me})_2]$ [**1**; $NSi^{Me} = (4\text{-methylpyridin-2-yl}oxy)dimethylsilyl]$ / $B(C_6F_5)_3$ promotes the selective reduction of CO_2 with tertiary silanes to the corresponding bis(silyl)acetal. Stoichiometric and catalytic studies evidenced that species $[Ir(CF_3COO-B(C_6F_5)_3)(\kappa^2-NSi^{Me})_2]$ (**3**), $[Ir(\kappa^2-NSi^{Me})_2][HB(C_6F_5)_3]$ (**4**), and $[Ir(HCOO-B(C_6F_5)_3)(\kappa^2-NSi^{Me})_2]$ (**5**) are intermediates of the catalytic process. The structure of **3** has been determined by X-ray diffraction methods. Theoretical calculations show that the rate-limiting step for the $1/B(C_6F_5)_3$ -catalyzed hydrosilylation of CO_2 to bis(silyl)acetal is a boron-promoted Si–H bond cleavage via an iridium silylacetate borane adduct.

The potential of CO_2 as a renewable and cheap C1 carbon source has received increasing attention over recent years.¹ The major difficulties to achieve this goal are the kinetic and thermodynamic stability of CO_2 , which hampers most of its chemical transformations. In this regard, catalysis has proven to be an essential tool for transforming CO_2 into value-added chemicals. Although great advances have been made in the field of the catalytic transformation of CO_2 , there are still many challenges to overcome for its utilization as a raw material on an industrial scale.^{2,3}

Formic acid, formaldehyde, methanol, and methane are C1 chemicals that can be obtained from the reduction of CO_2 . In this work, we focus on formaldehyde, which is obtained industrially by the partial oxidation of methanol and has an annual demand of 30 million tons.⁴ The catalytic hydrogenation of CO_2 to formaldehyde has been scarcely reported.⁵ However, several examples of the catalytic reduction of CO_2 to the formaldehyde level with hydrosilanes^{6–14} or hydroboranes¹⁵ have been reported. Catalytic systems based on Zr,⁶ Re,⁷ Ru,⁸ Co,⁹ Ni,¹⁰ Pd,¹¹ Pt,¹¹ Sc,¹² Mg,¹³ and Zn¹³ complexes and germylene- $B(C_6F_5)_3$ adducts¹⁴ have proven to be effective for the selective reduction of CO_2 with hydrosilanes to the corresponding bis(silyl)acetal. It is noteworthy that all of these catalytic systems require the use of a Lewis acid, such as $B(C_6F_5)_3$, to selectively achieve the formation of the corresponding bis(silyl)acetal.¹⁶ The selectivity of these processes depends on the metal/ $B(C_6F_5)_3$ ratio. Thus, with an excess of borane, the formation of methane is facilitated.^{6–14} Although the effectivity of $B(C_6F_5)_3$ as a hydrosilylation catalyst is well-known,¹⁷ $B(C_6F_5)_3$ alone cannot catalyze the hydrosilylation of CO_2 .^{6a,18}

It has recently been proven that bis(silyl)acetal, $H_2C(OSiPh_3)_2$, provides a means to incorporate CH_n ($n = 1$ or 2) moieties into organic molecules.¹⁹ Therefore, developing catalytic systems effective for the reduction of CO_2 to the bis(silyl)acetal level using hydrosilanes is of great interest.

To date, few studies have been reported on the mechanism of these processes. Indeed, the mechanistic discussion remains open. For example, two different mechanisms have been proposed for the bis(phosphino)borylnickel hydride/ $B(C_6F_5)_3$ -catalyzed reduction of CO_2 to the formaldehyde level with hydrosilanes. Thus, while Rodriguez et al. proposed a boron-promoted Si–H activation mechanism,^{10a,b} Ke et al. proposed a nickel-promoted Si–H mechanism.^{10c}

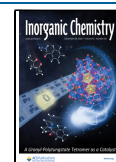
Understanding the mechanisms that operate in different transition-metal-catalyzed processes to reduce CO_2 with hydrosiloxanes is one of our aims.²⁰ We have recently reported that species $[Ir(CF_3CO_2)(\kappa^2-NSi^{Me})_2]$ [**1**; $NSi^{Me} = (4\text{-methylpyridin-2-yl}oxy)dimethylsilyl]$ catalyzes the selective reduction of CO_2 with $HSiMe(OSiMe_3)_2$ to the corresponding methoxysilane, $CH_3OSiMe(OSiMe_3)_2$, or silylformate, $HCO_2SiMe(OSiMe_3)_2$, under mild reaction conditions. The selectivity of this catalytic system can be easily tuned by controlling the pressure of CO_2 .²¹ It is noteworthy that the two active positions of the catalytic systems based on **1** are trans located to two silyl groups; in addition, the Ir–Si bond in such species is stronger than would be expected for a traditional Ir–silyl bond.²² Hence, the positions trans to the Ir–Si bonds in $Ir(\kappa^2-NSi^{Me})_2$ complexes are highly activated.

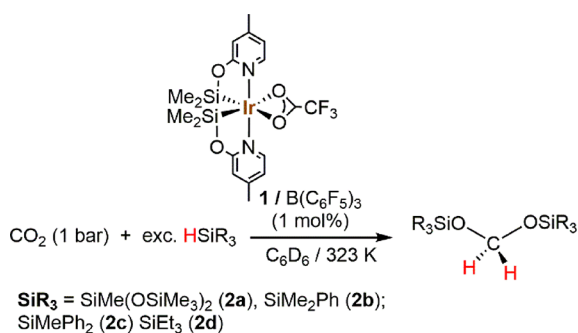
We now report that using **1** as a catalyst precursor in the presence of catalytic amounts of $B(C_6F_5)_3$ allow achievement of the selective formation of bis(silyl)acetals by the reaction of CO_2 with hydrosilanes (Scheme 1).

¹H NMR studies of the $1/B(C_6F_5)_3$ (1:1 ratio; 1.0 mol %)-catalyzed reaction of CO_2 (1 bar) with $HSiMe(OSiMe_3)_2$

Received: September 19, 2022

Published: December 6, 2022



Scheme 1. 1-Catalyzed (1.0 mol %) Reactions of CO₂ with Tertiary Silanes in the Presence of B(C₆F₅)₃ (1.0 mol %)


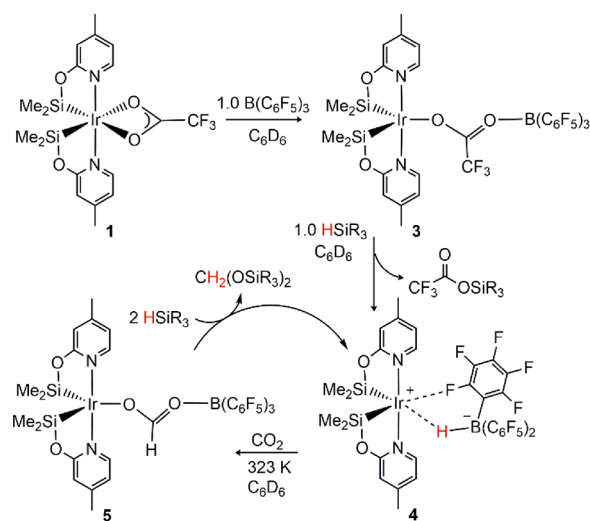
(HMTS) in C₆D₆ at 323 K show the slow and selective formation of H₂C{OSiMe(OSiMe₃)₂}₂ (**2a**; Table 1, entry 1). To explore the scope of this catalytic process, we performed the reaction of CO₂ with different silicon hydrides (HSiMe₂Ph, HSiMePh₂, HSiEt₃, and HSiMe(OSiMe₃)₂) in the presence of **1**/B(C₆F₅)₃ (1:1) in C₆D₆. The best reaction conditions were found to be CO₂ (1 bar) and 323 K. The reactions are highly selective to the formation of the corresponding bis(silyl)acetal (Table 1, entries 1, 2, 4, and 5). The nature of silane influences the reaction performance. The best reaction rates were obtained using HSiMe₂Ph and HSiMePh₂ (Table 1). The reactions with HMTS and HSiEt₃ were slower, which can be attributable to the higher hindrance of the Si–H bond in such compounds.

¹H NMR studies of the **1**/B(C₆F₅)₃ (1:1; 1.0 mol %)-catalyzed reaction of CO₂ with HSiMe₂Ph in C₆D₆ at 323 K demonstrate the influence of CO₂ pressure on the reaction performance; at 3 bar, the reactions are faster but less selective than those at 1 bar (Table 1, entries 2 and 6). The stoichiometry of borane is a key factor in the selectivity of these catalytic processes. Within the range of 1–3 bar of CO₂, if the load of B(C₆F₅)₃ is increased from 1.0 to 2.0 mol %, the reactions are selective toward the formation of methane²³ and O(SiMe₂Ph)₂, albeit at a lower rate (Table 1, entry 7). While reducing the amount of B(C₆F₅)₃ to 0.5 mol % does not alter the activity, the selectivity is affected, resulting in the formation of silylformate (82%) and bis(silyl)acetal (18%) as secondary

products (Table 1, entry 8). In the absence of additives, the catalyst precursor **1** promotes the reduction of CO₂ (1 bar) with HSiMe₂Ph to give silylformate (90%) as major reaction product (Table 1, entry 9).

¹H NMR studies of the **1**-catalyzed (1.0 mol %) reaction of CO₂ (1 bar) with HSiMe₂Ph in the presence of BPh₃ (1.0 mol %), instead of B(C₆F₅)₃, show a slower and less selective reaction. After 24 h, a 73% conversion of hydrosilane is reached to give a mixture of the corresponding silylformate (81%), bis(silyl)acetal (12%), and methoxysilane (7%) (Table 1, entry 3). Therefore, BPh₃ plays a role in the activity and selectivity of the process, although to a lesser degree than B(C₆F₅)₃, which can be correlated to its lower Lewis acidic character.²⁴

¹H NMR studies of the reaction of **1** with B(C₆F₅)₃ evidenced the quantitative formation of [Ir(CF₃COO-B(C₆F₅)₃)(κ²-NSi^{Me})₂] [**3** (CCDC 2218258)]; Scheme 2].

Scheme 2. NMR Monitoring of the Stepwise Stoichiometric Reaction


Contrarily, no reaction is observed between **1** and BPh₃ under the same conditions. The molecular structure of **3** has been confirmed by X-ray diffraction studies (Figure S38). The

Table 1. Results from the **1 (1.0 mol %)- and BR₃-Catalyzed Reaction of CO₂ with Hydrosilanes in C₆D₆ at 323 K**

entry	silane	borane	equiv of BR ₃	CO ₂ (bar)	time (h)	conversion (%) ^a	ratio of the reaction products			
							OCHO (%) ^b	OCH ₂ O (%) ^b	CH ₃ O (%) ^b	CH ₄ (%)
1	HMTS	B(C ₆ F ₅) ₃	1	1	16	28		>99	<1	
					40	74		>99	<1	
2	HSiMe ₂ Ph	B(C ₆ F ₅) ₃	1	1	16	93		>99	<1	
					40	>99		>99	<1	
3	HSiMe ₂ Ph	BPh ₃	1	1	24	73	81	12	7	
4	HSiMePh ₂	B(C ₆ F ₅) ₃	1	1	16	78		>99	<1	
					40	>99		>99	<1	
5	HSiEt ₃	B(C ₆ F ₅) ₃	1	1	16	12		>99	<1	
					40	25		>99	<1	
6	HSiMe ₂ Ph	B(C ₆ F ₅) ₃	1	3	8	>99	83	13	4	
7	HSiMe ₂ Ph	B(C ₆ F ₅) ₃	2	1	24	48				>99 ^c
8	HSiMe ₂ Ph	B(C ₆ F ₅) ₃	0.5	1	24	93	82	18		
9	HSiMe ₂ Ph			1	24	50	90	2	8	

^aConversion and selectivity percentages are based on ¹H NMR integration using hexamethylbenzene (0.0525 mmol) as an internal standard.

^bComposition of the mixture of products. ^cOn the basis of the ¹H NMR integral of O(SiMe₂Ph)₂, 12% CH₄ was formed.

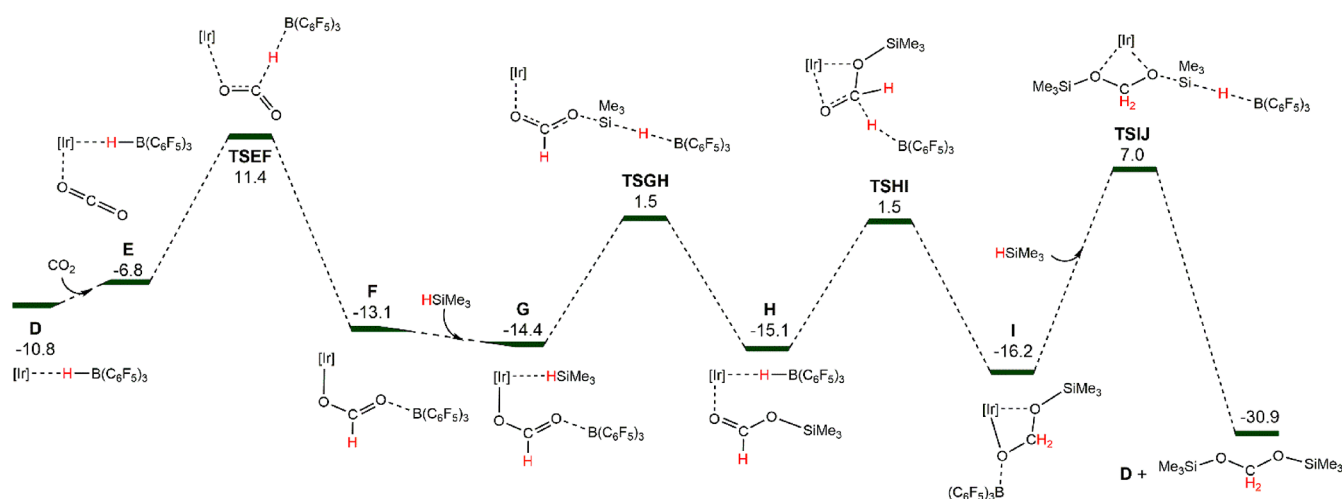


Figure 1. DFT-calculated Gibbs free energy profile for the catalytic formation of bis(silyl)acetal from E (kcal mol⁻¹) relative to A.

geometrical parameters of the [Ir(κ^2 -NSi^{Me})₂] fragment (see the Supporting Information, SI) agree with those of **1**, with short Ir–Si bond lengths [2.2526(11) and 2.2599(11) Å]. The Ir–O bond length in **3** [2.285(3) Å] is shorter than those found in **1** [2.363(3) and 2.418(3) Å].^{22a}

The ¹¹B{¹H} NMR spectra of **3** show a singlet at $\delta = -1.7$ ppm (Figure S18), in agreement with what is expected for the O–B(C₆F₅)₃ fragment²⁵ (Scheme 2). The absolute value of the difference between δ_{para} and δ_{meta} of the fluorine atoms $\Delta(\delta_{\text{m,p}})$ in the ¹⁹F NMR spectra of **3** is 6.3 ppm (Figure S21), which agrees with the presence of a tetracoordinated borate anion.^{26,27}

The addition of 1 equiv of HSiMe(OSiMe₃)₂ at room temperature (RT), to C₆D₆ solutions of **3** gives [Ir(κ^2 -NSi^{Me})₂][HB(C₆F₅)₃] (**4**) and CF₃CO₂SiR₃. The ¹¹B NMR spectra of **4** show a doublet resonance at $\delta = -15.1$ ppm (¹J_{B–H} = 53 Hz),^{12b,15a} which in the ¹¹B{¹H} NMR spectra appears as a singlet (Figures S24 and S25). Moreover, the ¹⁹F NMR spectra show a $\Delta(\delta_{\text{m,p}})$ value of ~ 6 ppm, which is higher than the characteristic values found for noncoordinating [HB(C₆F₅)₃][–] anions [$\Delta(\delta_{\text{m,p}}) < 3$ ppm], which indicates a certain degree of coordination of the [HB(C₆F₅)₃][–] anion to the metallic center.^{17b}

The addition of an excess of HSiMe(OSiMe₃)₂ to C₆D₆ solutions of **3** produces **4** and CF₃CH{OSiMe(OSiMe₃)₂}₂. Note that the overreduced product CF₃CH₂OSiMe(OSiMe₃)₂ is not obtained, which is reminiscent of the 1/B(C₆F₅)₃ system selectivity toward the bis(silyl)acetal species. This evidences the effective entrapment of B(C₆F₅)₃ in the form of a hydridoborate ion pair because the free borane might promote activation of the Si–H bond toward reduction of the bis(silyl)acetal derivatives, as well as the direct participation of **4** in the catalytic reaction, because **4** not only promotes hydrosilylation of the TFA ligand or CO₂ but also catalyzes reduction of the R'COOSiR₃ species (R' = H, CF₃).

The ¹H NMR spectra of **4** in C₆D₆ show no changes when pressurized with CO₂ (3 bar) at RT. However, after the reaction mixture is heated at 323 K, the formation of complex [Ir(HCOOB(C₆F₅)₃)(κ^2 -NSi^{Me})₂] (**5**) is observed. The presence of a IrOC(H)OB(C₆F₅)₃ moiety in **5** has been demonstrated by means of ¹H, ¹³C, ¹¹B, and ¹⁹F NMR spectroscopies (Figures S32–S36). The addition of 2 equiv of HSiMe(OSiMe₃)₂ to a solution of **5**, in the absence of CO₂,

produces the formation of **2a** and the regeneration of **4** within 1 h at RT (Scheme 2). Exposure of **5** to ¹³CO₂ (2.7 bar) at 353 K for 48 h did not result in the partial substitution of [Ir]OC(H)OB(C₆F₅)₃ to the ¹³C-enriched [Ir]O¹³C(H)OB(C₆F₅)₃, which suggests that, different from that reported for analogous MOC(H)OB(C₆F₅)₃ (M = Re,⁸ Ni,¹⁰ Pd,¹¹ Pt¹¹) species, the CO₂ insertion step to give **5** is irreversible under the catalytic conditions.

Density functional theory (DFT) studies at the M06L-(SMD)/def2-TZVP//B3LYP-D3(BJ)/def2-SVP level have been performed to study in detail the reaction mechanism of CO₂ hydrosilylation catalyzed by **3** (see the SI). HSiMe₃ has been selected as a model system for the silanes. The Gibbs free energy energetic profile for the catalyst activation process, from **3** (A) to **4** (D) (Figure S39), is exoergic by 10.8 kcal mol⁻¹. Si–H bond activation occurs via boron-promoted Si–H cleavage TSBC (9.0 kcal mol⁻¹), which corresponds to a linear S_N2 nucleophilic attack of the terminal oxygen of the trifluoroacetate ligand to the silicon atom in which the leaving hydride is transferred to the boron moiety. A similar type of activation mechanism has been proposed for Lewis acid PBP–Ni hydrosilylation of CO₂ based on DFT calculations.^{10b} An alternative mechanism for the Si–H activation step based on a nickel-promoted Si–H cleavage has been proposed.^{10c} In our case, the iridium-promoted Si–H cleavage is energetically disfavored (see Figures S40 and S41 for a comparison of both pathways). Intermediate **D** can be described as a hydroborate moiety and a cationic metallic complex rather than a metal hydride interacting with the Lewis acid. Inspection of the natural bond orbitals reveals a σ (B–H) bonding orbital with an electron population of 1.76 electrons (Figure S42).

The coordination of CO₂ to **D** leads to the beginning of the catalytic cycle. The Gibbs free energy profile for this process is reported in Figure 1. The first step corresponds to hydride transfer from HB(C₆F₅)₃ to CO₂ via TSEF at an energy barrier of 22.2 kcal mol⁻¹ from intermediate **D**. The obtained intermediate **F** is thermodynamically favored (–13.1 kcal mol⁻¹) and corresponds to complex **5** experimentally detected by NMR. Following that, the addition of silane leads to σ^1 -H-(HSiMe₃) coordination to **F**, yielding **G**. Then, activation of the Si–H bond takes place via TSGH, like the previously reported TSBC, consisting of the linear S_N2 nucleophilic attack of the terminal oxygen atom of the formate to the silicon atom

and transfer of the leaving hydride to the boron atom of the Lewis acid. The activation barrier of TSGH is $15.9 \text{ kcal mol}^{-1}$, leading to intermediate **H**. The subsequent hydride transfer from the hydroborate to the carbon atom of the silylformate coordinated to the metal takes place through TSHI, yielding intermediate **I**. Upon reaction with another molecule of HSiMe_3 , the silylformate develops into the final bis(silyl)acetal product via TSIJ, with the activation energy for this step being $23.2 \text{ kcal mol}^{-1}$. This activation barrier for the boron-promoted Si–H bond cleavage is higher than those of the previously related processes, TSBC ($9.0 \text{ kcal mol}^{-1}$) and TSGH ($15.9 \text{ kcal mol}^{-1}$). It should be noted that, for TSIJ, the nucleophilic attack to the silane is performed by an alkoxy group,^{10,17c,28} in contrast with previous steps, where the nucleophilic attack was performed by trifluoroacetate and formate groups.

The catalytic process is strongly exergonic ($-30.9 \text{ kcal mol}^{-1}$), and the rate-limiting step is boron-promoted Si–H cleavage by the iridium silylacetal borane adduct **I** ($23.2 \text{ kcal mol}^{-1}$) characterized by TSIJ. This activation barrier agrees with the experimental finding that the reaction proceeds slowly at RT. Indeed, the reaction of **4** with CO_2 (3 bar) to give **5** requires heating at 323 K. It should be noted that the intermediates proposed in the DFT-calculated catalytic cycle match the experimentally detected species (**4** and **5**; Scheme 2).

In conclusion, this is the first example of an iridium-based catalytic system effective for the selective reduction of CO_2 to the formaldehyde level with hydrosilanes. The selectivity of this catalytic system to the formation of bis(silyl)acetals is determined by the interaction between the active species and the Lewis acid $\text{B}(\text{C}_2\text{F}_6)_3$. In fact, any factor that affects that interaction influences the selectivity of the process. Thus, using a borane with a lower Lewis acidity such as BPh_3 , high temperature, or CO_2 pressure higher than 1.0 bar inhibit the selectivity toward the bis(silyl)acetal. DFT calculations support a boron-promoted Si–H cleavage mechanism, with the rate-limiting step being boron-promoted Si–H cleavage by the iridium silylacetal borane adduct **I**.

■ ASSOCIATED CONTENT

SI Supporting Information

The Supporting Information is available free of charge at <https://pubs.acs.org/doi/10.1021/acs.inorgchem.2c03330>.

Experimental details, NMR spectra, crystallographic, and theoretical calculation data (PDF)

Accession Codes

CCDC 2218258 contains the supplementary crystallographic data for this paper. These data can be obtained free of charge via www.ccdc.cam.ac.uk/data_request/cif, or by emailing data_request@ccdc.cam.ac.uk, or by contacting The Cambridge Crystallographic Data Centre, 12 Union Road, Cambridge CB2 1EZ, UK; fax: +44 1223 336033.

■ AUTHOR INFORMATION

Corresponding Author

Francisco J. Fernández-Alvarez – Facultad de Ciencias, Departamento de Química Inorgánica, Instituto de Síntesis Química y Catálisis Homogénea, Universidad de Zaragoza, CSIC, Zaragoza 50009, Spain; orcid.org/0000-0002-0497-1969; Email: paco@unizar.es

Authors

Jefferson Guzmán – Facultad de Ciencias, Departamento de Química Inorgánica, Instituto de Síntesis Química y Catálisis Homogénea, Universidad de Zaragoza, CSIC, Zaragoza 50009, Spain

Asier Urriolabeitia – Facultad de Ciencias, Departamento de Química Física, BIFI, Universidad de Zaragoza, Zaragoza 50009, Spain; orcid.org/0000-0001-9352-6922

Marina Padilla – Facultad de Ciencias, Departamento de Química Inorgánica, Instituto de Síntesis Química y Catálisis Homogénea, Universidad de Zaragoza, CSIC, Zaragoza 50009, Spain

Pilar García-Orduña – Facultad de Ciencias, Departamento de Química Inorgánica, Instituto de Síntesis Química y Catálisis Homogénea, Universidad de Zaragoza, CSIC, Zaragoza 50009, Spain

Victor Polo – Facultad de Ciencias, Departamento de Química Física, BIFI, Universidad de Zaragoza, Zaragoza 50009, Spain; orcid.org/0000-0001-5823-7965

Complete contact information is available at:

<https://pubs.acs.org/doi/10.1021/acs.inorgchem.2c03330>

Author Contributions

J.G., M.P., and F.J.F.-A., experimental studies; P.G.-O., X-ray diffraction; A.U. and V.P., theoretical calculations.

Notes

The authors declare no competing financial interest.

■ ACKNOWLEDGMENTS

Financial support from Projects PGC2018-099383-B-I00 (MCIU/AEI/FEDER, UE) and DGA/FSE Project E42_20R is gratefully acknowledged. A.U. thankfully acknowledges the Spanish MECED for a FPU fellowship (FPU 2017/05417). The authors acknowledge the resources from the supercomputers “Memento” and “Cierzo” and technical expertise and assistance provided by BIFI-ZCAM (Universidad de Zaragoza, Spain). M.P. thankfully acknowledges the resources cofinanced with the European Social Fund (ESF) and the Youth Employment Initiative assigned to the CSIC in the Youth Employment Operational Program ESF 2014-2020.

■ REFERENCES

- (1) (a) Artz, J.; Müller, T. E.; Thenert, K.; Kleinekorte, J.; Meys, R.; Sternberg, A.; Bardow, A.; Leitner, W. Sustainable Conversion of Carbon Dioxide: An Integrated Review of Catalysis and Life Cycle Assessment. *Chem. Rev.* **2018**, *118*, 434–504. (b) Stahel, W. R. The circular economy. *Nature* **2016**, *531*, 435–438. (c) Clark, J. H.; Farmer, T. J.; Herrero-Davila, L.; Sherwood, J. Circular economy design considerations for research and process development in the chemical sciences. *Green Chem.* **2016**, *18*, 3914–3934. (d) Grignard, B.; Gennen, S.; Jérôme, C.; Kleij, A. W.; Detrembleur, C. Advances in the use of CO_2 as a renewable feedstock for the synthesis of polymers. *Chem. Soc. Rev.* **2019**, *48*, 4466–4514. (e) Martens, J. A.; Bogaerts, A.; De Kimpe, N.; Jacobs, P. A.; Marin, G. B.; Rabaey, K.; Saeys, M.; Verhelst, S. The Chemical Route to a Carbon Dioxide Neutral World. *ChemSusChem* **2017**, *10*, 1039–1055.
- (2) For some reviews, see: (a) Liu, Q.; Wu, L.; Jackstell, R.; Beller, M. Using carbon dioxide as a building block in organic synthesis. *Nat. Commun.* **2015**, *6*, 5933. (b) Wang, W.-H.; Himeda, Y.; Muckerman, J. T.; Manbeck, G. F.; Fujita, E. CO_2 Hydrogenation to Formate and Methanol as an Alternative to Photo- and Electrochemical CO_2 Reduction. *Chem. Rev.* **2015**, *115*, 12936–12973. (c) Aresta, M.; Dibenedetto, A.; Angelini, A. Catalysis for the Valorization of Exhaust Carbon: from CO_2 to Chemicals, Materials, and Fuels. *Technological*

- Use of CO₂. *Chem. Rev.* **2014**, *114*, 1709–1742. (d) Das Neves Gomes, C.; Jacquet, O.; Villiers, C.; Thuéry, P.; Ephritikhine, M.; Cantat, T. A Diagonal Approach to Chemical Recycling of Carbon Dioxide: Organocatalytic Transformation for the Reductive Functionalization of CO₂. *Angew. Chem., Int. Ed.* **2012**, *51*, 187–190. (e) Cokoja, M.; Bruckmeier, C.; Rieger, B.; Herrmann, W. A.; Kühn, F. E. Transformation of Carbon Dioxide with Homogeneous Transition-Metal Catalysts: A Molecular Solution to a Global Challenge? *Angew. Chem., Int. Ed.* **2011**, *50*, 8510–8537. (f) Peters, M.; Köhler, B.; Kuckshinrichs, W.; Leitner, W.; Markewitz, P.; Müller, T. E. Chemical Technologies for Exploiting and Recycling Carbon Dioxide into the Value Chain. *ChemSusChem* **2011**, *4*, 1216–1240. (g) Wang, W.; Wang, S.; Ma, X.; Gong, J. Recent advances in catalytic hydrogenation of carbon dioxide. *Chem. Soc. Rev.* **2011**, *40*, 3703–3727. (h) Sakakura, T.; Choi, J.-C.; Yasuda, H. Transformation of Carbon Dioxide. *Chem. Rev.* **2007**, *107*, 2365–2387. (i) Jessop, P. G.; Joó, F.; Tai, C.-C. Recent advances in the homogeneous hydrogenation of carbon dioxide. *Coord. Chem. Rev.* **2004**, *248*, 2425–2442. (j) Jessop, P. G.; Ikariya, T.; Noyori, R. Homogeneous Hydrogenation of Carbon Dioxide. *Chem. Rev.* **1995**, *95*, 259–272.
- (3) For recent reviews on the catalytic hydrogenation of CO₂, see: (a) Ronda-Lloret, M.; Rothenberg, G.; Shiju, N. R. A Critical Look at Direct Catalytic Hydrogenation of Carbon Dioxide to Olefins. *ChemSusChem* **2019**, *12*, 3896–3914. (b) Onishi, N.; Laurenczy, G.; Beller, M.; Himeda, Y. Recent progress for reversible homogeneous catalytic hydrogen storage in formic acid and in methanol. *Coord. Chem. Rev.* **2018**, *373*, 317–332. (c) Jia, J.; Qian, C.; Dong, Y.; Li, Y. F.; Wang, H.; Ghossoub, M.; Butler, K. T.; Walsh, A.; Ozin, G. A. Heterogeneous catalytic hydrogenation of CO₂ by metal oxides: defect engineering – perfecting imperfection. *Chem. Soc. Rev.* **2017**, *46*, 4631–4644.
- (4) (a) Heim, L. E.; Konnerth, H.; Precht, M. H. G. Future perspectives for formaldehyde: pathways for reductive synthesis and energy storage. *Green Chem.* **2017**, *19*, 2347–2355. (b) Bahmanpour, A. M.; Hoadley, A.; Mushrif, S. H.; Tanksale, A. Hydrogenation of carbon monoxide into formaldehyde in liquid media. *ACS Sustainable Chem. Eng.* **2016**, *4*, 3970–3977. (c) Desmons, S.; Fauré, R.; Bontemps, S. Formaldehyde as a promising C1 source: The instrumental role of biocatalysis for stereocontrolled reactions. *ACS Catal.* **2019**, *9*, 9575–9588.
- (5) Klankermayer, J.; Wesselbaum, S.; Beydoun, K.; Leitner, W. Selective catalytic synthesis using the combination of carbon dioxide and hydrogen: catalytic chess at the interface of energy and chemistry. *Angew. Chem., Int. Ed.* **2016**, *55*, 7296–7343.
- (6) (a) Matsuo, T.; Kawaguchi, H. From Carbon Dioxide to Methane: Homogeneous Reduction of Carbon Dioxide with Hydrosilanes Catalyzed by Zirconium–Borane Complexes. *J. Am. Chem. Soc.* **2006**, *128*, 12362–12363. (b) Luconi, L.; Rossin, A.; Tuci, G.; Gafurov, Z.; Lyubov, D. M.; Trifonov, A. A.; Cicchi, S.; Ba, H.; Pham-Huu, C.; Yakhvarov, D.; Giambastiani, G. Benzoimidazole-Pyridylamido Zirconium and Hafnium Alkyl Complexes as Homogeneous Catalysts for Tandem Carbon Dioxide Hydrosilylation to Methane. *ChemCatChem* **2019**, *11*, 495–510.
- (7) (a) Jiang, Y.; Blacque, O.; Fox, T.; Berke, H. Catalytic CO₂ Activation Assisted by Rhenium Hydride/B(C₆F₅)₃ Frustrated Lewis Pairs—Metal Hydrides Functioning as FLP Bases. *J. Am. Chem. Soc.* **2013**, *135*, 7751–7760. (b) Morris, D. S.; Weetman, C.; Wennmacher, J. T. C.; Cokoja, M.; Drees, M.; Kühn, F. E.; Love, J. B. Reduction of carbon dioxide and organic carbonyls by hydrosilanes catalysed by the perchlorate anion. *Catal. Sci. Technol.* **2017**, *7*, 2838–2845.
- (8) Metsänen, T. T.; Oestreich, M. Temperature-Dependent Chemoselective Hydrosilylation of Carbon Dioxide to Formaldehyde or Methanol Oxidation State. *Organometallics* **2015**, *34*, 543–546.
- (9) (a) Cramer, H. H.; Chatterjee, B.; Weyhermüller, T.; Werlé, C.; Leitner, W. Controlling the Product Platform of Carbon Dioxide Reduction: Adaptive Catalytic Hydrosilylation of CO₂ Using a Molecular Cobalt(II) Triazine Complex. *Angew. Chem., Int. Ed.* **2020**, *59*, 15674–15681. (b) Cramer, H. H.; Ye, S.; Neese, F.; Werlé, C.; Leitner, W. Cobalt-Catalyzed Hydrosilylation of Carbon Dioxide to the Formic Acid, Formaldehyde, and Methanol Level-How to Control the Catalytic Network? *JACS Au* **2021**, *1*, 2058–2069.
- (10) (a) Ríos, P.; Curado, N.; López-Serrano, J.; Rodríguez, A. Selective reduction of carbon dioxide to bis(silyl)acetal catalyzed by a PBP-supported nickel complex. *Chem. Commun.* **2016**, *52*, 2114–2117. (b) Ríos, P.; Rodríguez, A.; López-Serrano, J. Mechanistic Studies on the Selective Reduction of CO₂ to the Aldehyde Level by a Bis(phosphino)boryl (PBP)-Supported Nickel Complex. *ACS Catal.* **2016**, *6*, 5715–5723. (c) Huang, X.; Zhang, K.; Shao, Y.; Li, Y.; Gu, F.; Qu, L.-B.; Zhao, C.; Ke, Z. Mechanism of Si–H Bond Activation for Lewis Acid PBP-Ni-Catalyzed Hydrosilylation of CO₂: The Role of the Linear S_N2 Type Cooperation. *ACS Catal.* **2019**, *9*, 5279–5289.
- (11) Mitton, S. J.; Turculet, L. Mild Reduction of Carbon Dioxide to Methane with Tertiary Silanes Catalyzed by Platinum and Palladium Silyl Pincer Complexes. *Chem. Eur. J.* **2012**, *18*, 15258–15262.
- (12) (a) LeBlanc, F. A.; Piers, W. E.; Parvez, M. Selective Hydrosilylation of CO₂ to a Bis(silyl)acetal Using an Anilido Bipyridyl-Ligated Organoscandium Catalyst. *Angew. Chem., Int. Ed.* **2014**, *53*, 789–792. (b) Beh, D. W.; Piers, W. E.; Gelfand, B. S.; Lin, J.-B. Tandem deoxygenative hydrosilylation of carbon dioxide with a cationic scandium hydridoborate and B(C₆F₅)₃. *Dalton Trans* **2020**, *49*, 95–101.
- (13) Rauch, M.; Parkin, G. Zinc and Magnesium Catalysts for the Hydrosilylation of Carbon Dioxide. *J. Am. Chem. Soc.* **2017**, *139*, 18162–18165.
- (14) Del Rio, N.; Lopez-Reyes, M.; Baceiredo, A.; Saffon-Merceron, N.; Lutters, D.; Müller, T.; Kato, T. *N,P*-Heterocyclic Germylene/B(C₆F₅)₃ Adducts: A Lewis Pair with Multi-reactive Sites. *Angew. Chem., Int. Ed.* **2017**, *56*, 1365–1370.
- (15) For some recent examples of the catalytic hydroboration of CO₂, see: (a) Anker, M. D.; Arrowsmith, M.; Bellham, P.; Hill, M. S.; Kociok-Köhne, G.; Liptrot, D. J.; Mahon, M. F.; Weetman, C. Selective reduction of CO₂ to a methanol equivalent by B(C₆F₅)₃-activated alkaline earth catalysis. *Chem. Sci.* **2014**, *5*, 2826–2830. (b) Murphy, L. J.; Hollenhorst, H.; McDonald, R.; Ferguson, M.; Lumsden, M. D.; Turculet, L. Selective Ni-Catalyzed Hydroboration of CO₂ to the Formaldehyde Level Enabled by New PSiP Ligation. *Organometallics* **2017**, *36*, 3709–3720. (c) Espinosa, M. R.; Charboneau, D. J.; Garcia de Oliveira, A.; Hazari, N. Controlling Selectivity in the Hydroboration of Carbon Dioxide to the Formic Acid, Formaldehyde, and Methanol Oxidation Levels. *ACS Catal.* **2019**, *9*, 301–314. (d) Wang, X.; Chang, K.; Xu, X. Hydroboration of carbon dioxide enabled by molecular zinc dihydrides. *Dalton Trans* **2020**, *49*, 7324–7327. (e) Zhang, L.; Zhao, Y.; Liu, C.; Pu, M.; Lei, M.; Cao, Z. *Inorg. Chem.* **2022**, *61*, 5616–5625.
- (16) (a) Ríos, P.; Rodríguez, A.; Conejero, S. Activation of Si–H and B–H bonds by Lewis acidic transition metals and p-block elements: same, but different. *Chem. Sci.* **2022**, *13*, 7392–7418. (b) Stahl, T.; Hrobárik, P.; Königs, C. D. F.; Ohki, Y.; Tatsumi, K.; Kemper, S.; Kaupp, M.; Klare, H. F. T.; Oestreich, M. Mechanism of the cooperative Si–H bond activation at Ru–S bonds. *Chem. Sci.* **2015**, *6*, 4324–4334.
- (17) (a) Parks, D. J.; Piers, W. E. Tris(pentafluorophenyl)boron-Catalyzed Hydrosilylation of Aromatic Aldehydes, Ketones, and Esters. *J. Am. Chem. Soc.* **1996**, *118*, 9440–9441. (b) Parks, D. J.; Blackwell, J. M.; Piers, W. E. Studies on the Mechanism of B(C₆F₅)₃-Catalyzed Hydrosilylation of Carbonyl Functions. *J. Org. Chem.* **2000**, *65*, 3090–3098. (c) Hog, D. T.; Oestreich, M. B(C₆F₅)₃-Catalyzed Reduction of Ketones and Imines Using Silicon-Stereogenic Silanes: Stereoreduction by Single-Point Binding. *Eur. J. Org. Chem.* **2009**, *2009*, 5047–5056. (d) Houghton, A. Y.; Hurlmalainen, J.; Mansikkamäki, A.; Piers, W. A.; Tuononen, H. M. Direct observation of a borane-silane complex involved in frustrated Lewis-pair-mediated hydrosilylations. *Nat. Chem.* **2014**, *6*, 983–988. (e) Oestreich, M.; Hermeke, J.; Mohr, J. A unified survey of Si–H and H–H bond activation catalysed by electron-deficient boranes. *Chem. Soc. Rev.* **2015**, *44*, 2202–2220. (f) Keess, S.; Simonneau, A.; Oestreich, M. Direct and Transfer Hydrosilylation Reactions Catalyzed by Fully or

Partially Fluorinated Triarylboranes: A Systematic Study. *Organometallics* **2015**, *34*, 790–799.

(18) Berkefeld, A.; Piers, W. E.; Parvez, M. Tandem Frustrated Lewis Pair/Tris(pentafluorophenyl)borane-Catalyzed Deoxygenative Hydrosilylation of Carbon Dioxide. *J. Am. Chem. Soc.* **2010**, *132*, 10660–10661.

(19) Rauch, M.; Strater, Z.; Parkin, G. Selective Conversion of Carbon Dioxide to Formaldehyde via a Bis(silyl)acetal: Incorporation of Isotopically Labeled C1 Moieties Derived from Carbon Dioxide into Organic Molecules. *J. Am. Chem. Soc.* **2019**, *141*, 17754–17762.

(20) (a) Lalrempuia, R.; Iglesias, M.; Polo, V.; Sanz Miguel, P. J.; Fernández-Alvarez, F. J.; Pérez-Torrente, J. J.; Oro, L. A. Effective Fixation of CO₂ by Iridium-Catalyzed Hydrosilylation. *Angew. Chem., Int. Ed.* **2012**, *51*, 12824–12827. (b) Julián, A.; Jaseer, E. A.; Garcés, K.; Fernández-Alvarez, F. J.; García-Orduña, P.; Lahoz, F. J.; Oro, L. A. Tuning the activity and selectivity of iridium-NSiN catalyzed CO₂ hydrosilylation processes. *Catal. Sci. Technol.* **2016**, *6*, 4410–4417. (c) Julián, A.; Guzmán, J.; Jaseer, E. A.; Fernández-Alvarez, F. J.; Royo, R.; Polo, V.; García-Orduña, P.; Lahoz, F. J.; Oro, L. A. Mechanistic Insights on the Reduction of CO₂ to Silylformates Catalyzed by Ir-NSiN Species. *Chem. Eur. J.* **2017**, *23*, 11898–11907.

(21) Guzmán, J.; García-Orduña, P.; Polo, V.; Lahoz, F. J.; Oro, L. A.; Fernández-Alvarez, F. J. Ir-catalyzed selective reduction of CO₂ to the methoxy or formate level with HSiMe(OSiMe₃)₂. *Catal. Sci. Technol.* **2019**, *9*, 2858–2867.

(22) (a) Guzmán, J.; Bernal, A. M.; García-Orduña, P.; Lahoz, F. J.; Polo, V.; Fernández-Alvarez, F. J. 2-Pyridone-stabilized iridium silylene/silyl complexes: structure and QTAIM analysis. *Dalton Trans* **2020**, *49*, 17665–17673. (b) García-Orduña, P.; Fernández, I.; Oro, L. A.; Fernández-Alvarez, F. J. Origin of the Ir–Si bond shortening in Ir–NSiN complexes. *Dalton Trans* **2021**, *50*, 5951–5959. (c) Gómez-España, A.; García-Orduña, P.; Guzmán, J.; Fernández, I.; Fernández-Alvarez, F. J. Synthesis and Characterization of Ir(κ^2 -NSi) Species Active toward the Solventless Hydrolysis of HSiMe(OSiMe₃)₂. *Inorg. Chem.* **2022**, *61*, 16282–16294.

(23) The selective formation of ¹³CH₄ was confirmed by ¹³C labeling using ¹³CO₂ (Figure S37).

(24) Mayer, R. J.; Hampel, N.; Ofial, A. R. Lewis Acidic Boranes. Lewis bases, and Equilibrium Constants: A Reliable Scaffold for a Quantitative Lewis Acidity/Basicity Scale. *Chem. Eur. J.* **2021**, *27*, 4070–4080.

(25) Bibal, C.; Santini, C. C.; Chauvin, Y.; Vallée, C.; Olivier-Bourbigou, H. A selective synthesis of hydroxyborate anions as novel anchors for zirconocene catalysts. *Dalton Trans* **2008**, 2866–2870.

(26) (a) Hayes, P. G.; Xu, Z.; Beddie, C.; Keith, J. M.; Hall, M. B.; Tilley, T. D. The Osmium–Silicon Triple Bond: Synthesis, Characterization, and Reactivity of an Osmium Silylyne Complex. *J. Am. Chem. Soc.* **2013**, *135*, 11780–11783. (b) Berkefeld, A.; Piers, W. E.; Parvez, M.; Castro, L.; Maron, L.; Eisenstein, O. Decamethyls-candocinium-hydrido-(perfluorophenyl)borate: fixation and tandem tris(perfluorophenyl)borane catalyzed deoxygenative hydrosilylation of carbon dioxide. *Chem. Sci.* **2013**, *4*, 2152–2162. (c) Horton, A. D. Direct Observation of β -Methyl Elimination in Cationic Neopentyl Complexes: Ligand Effects on the Reversible Elimination of Isobutene. *Organometallics* **1996**, *15*, 2675–2677.

(27) (a) Agnew, D. W.; Moore, C. E.; Rheingold, A. L.; Figueroa, J. S. Controlled *cis* Labilization of CO from Manganese(I) Mixed Carbonyl/Isocyanide Complexes: An Entry Point to Coordinatively Unsaturated Metallo-Lewis Acids. *Organometallics* **2017**, *36*, 363–371. (b) Beh, D. W.; Piers, W. E.; del Rosal, I.; Maron, L.; Gelfand, B. S.; Gendy, C.; Lin, J.-B. Scandium alkyl and hydride complexes supported by a pentadentate diborane ligand: reactions with CO₂ and N₂O. *Dalton Trans* **2018**, *47*, 13680–13688.

(28) (a) Robert, T.; Oestreich, M. Si-H Bond Activation: Bridging Lewis Acid Catalysis with Brookhart's Iridium (III) Pincer Complex and B(C₆F₅)₃. *Angew. Chem., Int. Ed.* **2013**, *52*, 5216–5218. (b) Metsänen, T. T.; Hrobárik, P.; Klare, H. F. T.; Kaupp, M.; Oestreich, M. Insight into the Mechanism of Carbonyl Hydro-

silylation Catalyzed by Brookhart's Iridium (III) Pincer Complex. *J. Am. Chem. Soc.* **2014**, *136*, 6912–6915.

Recommended by ACS

PCP Pincer Carbene Nickel(II) Chloride, Hydride, and Thiolate Complexes: Hydrosilylation of Aldehyde, Ketone, and Nitroarene by the Thiolate Complex

Ashok Kumar, Ganesan Mani, *et al.*

APRIL 05, 2023

ORGANOMETALLICS

READ 

Lewis Base Activation by Uranium(III) Complexes

Nathan J. Lin, Suzanne C. Bart, *et al.*

APRIL 10, 2023

ORGANOMETALLICS

READ 

Stable Silapyramidanes

Taiki Imagawa, David Scheschke, *et al.*

FEBRUARY 14, 2023

JOURNAL OF THE AMERICAN CHEMICAL SOCIETY

READ 

Pincer Platinum(II) Hydrides: High Stability Imparted by Donor-Flexible Pyridylidene Amide Ligands and Evidence for Adduct Formation before Protonation

Alexander J. Bukvic, Martin Albrecht, *et al.*

JANUARY 31, 2023

INORGANIC CHEMISTRY

READ 

Get More Suggestions >